*Molecular Simulation*
Vol. 38, Nos. 8–9, July–August 2012, 631–641



# Water in metal-organic frameworks: structure and diffusion of $H_2O$ in MIL-53(Cr) from quantum simulations

Francesco Paesani*

*Department of Chemistry and Biochemistry, University of California, San Diego, 9500 Gilman Drive, La Jolla, CA 92093, USA*

(*Received 18 December 2011; final version received 21 March 2012*)

The structural and dynamical properties of water in the nanopores of the MIL-53(Cr) metal-organic framework are examined using classical and quantum molecular dynamics simulations. The results indicate that, depending on the number of molecules adsorbed per unit cell as well as on the shape of the nanopores, the explicit inclusion of nuclear quantum effects can either enhance or inhibit the molecular mobility. At low loadings, when MIL-53(Cr) exists in a narrow pore configuration, the translational and rotational motion of the water molecules is largely suppressed. Importantly, it is found that nuclear quantum effects make the reorientation of the water molecules within the narrow nanopores slower than in the classical limit. This is attributed to the quantum delocalisation that effectively increases the molecular volume and, consequently, reduces the free space available in the nanopores. As the number of molecules per unit cell increases and the nanopores start opening, the dynamics of quantum water becomes faster again. Independent of the loading, the molecular mobility in MIL-53(Cr) is reduced with respect to bulk water.

**Keywords:** water; metal-organic frameworks; quantum effects

**Francesco Paesani** received his Ph.D. in Theoretical Physical Chemistry from the University of Rome "La Sapienza", Italy. From 2002 to 2005, he was a postdoctoral fellow at the University of California, Berkeley, working with Professor Birgitta Whaley. His research focused on the spectroscopy and superfluid behavior of helium droplets at low temperature. Subsequently, he was a postdoctoral researcher in the group of Professor Gregory Voth at the University of Utah working on the development of theoretical and computational methodologies for the investigation of structural, thermodynamic and dynamical properties of many-body systems at a quantum-mechanical level. Since 2009, he has been an Assistant Professor in the Department of Chemistry and Biochemistry at the University of California, San Diego. His research interests are focused on the theoretical and computational modeling of chemical processes at complex interfaces. He is also an active developer of the AMBER suite of codes for molecular dynamics simulations.

## 1. Introduction

Metal-organic frameworks (MOFs) are a relatively new class of nanoporous materials made of inorganic and organic subunits (or building blocks) where the organic molecules act as linkers between metal-based nodes to form 3D coordination networks [1]. Since an essentially infinite number of building blocks can be synthesised, a myriad of different MOF structures have been prepared. In contrast to traditional porous materials such as zeolites, many MOFs are characterised by unusually flexible frameworks that undergo reversible structural deformations (the so-called 'breathing behaviour') upon external stimuli such as temperature or pressure changes and gas adsorption [2–11]. It has recently been shown that the breathing behaviour of MOFs can also be modulated by chemical functionalisation of the framework [12,13].

Because of their unique properties related to chemical diversity, high surface area, porosity and stability, MOFs hold great promise for potential applications in gas storage, separations, catalysis, sensing, nonlinear optics, luminescence and magnetism [11,14–16]. However, before MOFs can actually find practical use in large-scale applications, it is of critical importance to determine their stability under realistic conditions. This implies that a detailed analysis at the molecular level of the impact of water adsorption on the overall physicochemical properties of the frameworks is required.

*Email: fpaesani@ucsd.edu

ISSN 0892-7022 print/ISSN 1029-0435 online

http://dx.doi.org/10.1080/08927022.2012.679620
http://www.tandfonline.com

The behaviour of MOFs under hydrated conditions displays a large degree of variability. Some frameworks degrade irreversibly due to the interaction with $H_2O$ molecules under mild conditions [17] while other structures remain highly stable even when completely immersed in water [18,19]. Experimental measurements indicate that MOF-177 can adsorb up to 10 wt% $H_2O$ at room temperature but decomposes after being exposed to moisture for 3 days [20]. Water adsorption isotherms at 303 K have been reported for water-resistant 3D pillared-layer MOFs [21], while analogous measurements show that both HKUST-1 (also known as CuBTC) and DUT-4 materials become unstable when put in direct contact with water [22]. By contrast, both Materials of Institut Lavoisier (MIL) and zeolitic imidazolate frameworks (ZIF) materials show high stability under hydrated conditions [22]. In general, the stability of MOFs in steam under different conditions of saturation and temperature correlates with the estimated dissociation energy of the metal–ligand bond [23]. In this regard, molecular dynamics (MD) simulations with classical force fields suggested that the displacement of the 1,4-benzenedicarboxylate (BDC) organic linkers coordinated to the Zn atoms in MOF-5 (also known as IRMOF-1) is likely involved in the dissociation process [17]. Subsequent simulations performed with an empirically parameterised reactive force field instead indicated that water hydrolysis promoted by direct interactions of $H_2O$ molecules with the Zn atoms of the framework is responsible for the collapse of the MOF-5 structure [24]. Interestingly, the decomposition under hydrated conditions of DABCO MOF (DMOF-1), which is structurally related to MOF-5, appears to occur via a different mechanism that involves the removal of the 1,4-diazabicyclo[2,2,2]octane (DABCO) pillars [25]. Although the presence of water in general limits the adsorption of other guest molecules, it has also been reported that the hydration of open metal sites in the CuBTC framework increases the amount of $CO_2$ that can be adsorbed under mild conditions relative to the dehydrated material [26,27].

Besides practical implications, the study of water in the MOF nanopores is also of fundamental importance for understanding how the thermodynamic properties, phase behaviour and molecular mobility of water change upon confinement depending on the properties of the substrate material (e.g. see Refs [28,29] and reference therein). The modifications of the short-range order in the liquid depend on the nature of the water–substrate interaction as well as on the spatial range and geometry of the substrate. In particular, it has been shown that the interaction with the substrate significantly perturbs the hydrogen bond (HB) network of water leading to large changes in the freezing and melting properties [30]. In this context, due to their chemical diversity, MOFs offer a unique opportunity to investigate the behaviour of water in confined environments where regions with different levels of hydrophilicity and hydrophobicity are present. A molecular-level understanding of how the highly connected HB network found in bulk is modified when water is confined in small cavities has broad implications in different areas, including heterogeneous catalysis, oil recovery and the characterisation of the stability and enzymatic activity of biomolecules.

Despite recent progress achieved through both experimental and computational studies, a complete understanding of the behaviour of water in confined environments still remains elusive. In this regard, the role played by nuclear quantum effects in determining the structural and dynamical properties of the water molecules adsorbed in nanopores has received little attention. By contrast, different experimental techniques and computer simulations have been used to investigate the role of nuclear quantum effects in bulk water (e.g. see Ref. [31] for a recent review). Using molecular simulations, it has been shown that the explicit inclusion of the quantisation of the nuclear motion results in a less structured HB network. This is accompanied by faster molecular diffusion and orientational dynamics, which can be directly related to zero-point energy contributions and possible tunneling effects [32].

Here, we report on molecular-level computer simulations carried out to investigate the structure and dynamics of water in MIL-53(Cr). MIL-53(Cr) is a 3D MOF with chemical formula $Cr(OH)[O_2C–C_6H_4–CO_2]$, which is built-up from infinite chains of corner-sharing $CrO_4(OH)_2$ clusters interconnected by terephthalate linkers [33]. MIL-53(Cr) belongs to the family of MOFs that breathe when exposed to external stimuli [3,4,34–39]. In particular, it has been shown that MIL-53(Cr) undergoes a transition from a large to a narrow pore structure and back to a large pore structure as a function of the number of water molecules adsorbed per unit cell [3,37].

The paper is organised as follows: the computational approach is presented in Section 2, the results are discussed in Section 3 and the conclusions are given in Section 4.

## 2. Computational methodology

Normal-mode path-integral molecular dynamics (NMPIMD) [40] was used to calculate the structural and thermodynamic properties of water at the quantum-mechanical level while the corresponding dynamical properties were obtained from centroid molecular dynamics (CMD) simulations [41]. Since both methods and their applications to water have been described in detail in a recent review [31], only a brief summary of the main concepts and numerical details specific to this study is provided here. NMPIMD is a numerically exact method that enables the calculation of structural and thermodynamic properties of a quantum system based upon

Feynman's formulation of statistical mechanics in terms of path integrals [42,43]. CMD is an approximate method for the calculation of the real-time dynamics of a quantum system in the condensed phase [44–50]. Within the CMD framework, the quantum dynamics of a system is described in terms of classical-like equations of motion applied to the centroid variables, where the centroids correspond to the centres of mass of the ring polymers representing the quantum particles according to the path-integral formalism. The CMD time propagation provides an efficient means to compute quantum time-correlation functions that can be used to determine the dynamical properties of a condensed phase system within linear response theory. Classical MD simulations in the constant stress and constant temperature (NσT), constant temperature and constant volume (NVT) and constant energy (NVE) ensembles [51,52] were also carried out in order to assess the differences between a classical and a quantum description of the system as well as to determine the impact of nuclear quantum effects on the behaviour of water adsorbed in the nanopores.

A periodic model of MIL-53(Cr) consisting of 32 unit cells was built following Ref. [37]. In all simulations, both the intra-framework and water–framework interactions were described by classical force fields. For the framework, we adopted the flexible force field developed in Ref. [37], which was shown to accurately reproduce the breathing behaviour of MIL-53(Cr) upon adsorption of $CO_2$, $H_2S$ and $H_2O$ [37–39]. The water interactions were described by the flexible q-SPC/Fw model that was specifically parameterised to reproduce the quantum properties of water at ambient conditions [53]. The Lorentz–Berthelot mixing rules were used to determine the van der Waals parameters associated with the framework–water interactions [51].

In both NMPIMD and CMD simulations, each atom was represented by a ring polymer with $P = 24$ beads, which was shown to be sufficient to capture nuclear quantum effects in water with the q-SPC/Fw model [53]. Classical simulations were instead carried out with $P = 1$. Different water loadings ($N_{H_2O}$) from 1 to 20 $H_2O$ molecules per unit cell were considered and the temperature was fixed at $T = 298$ K. For each loading, the water molecules were initially distributed uniformly in the nanopores, and each system was allowed to relax during a MD simulation of 1 ns carried out in the NσT ensemble. In these calculations, temperature and pressure were maintained using Nosé–Hoover thermostat and barostat with relaxation times of 1 and 5 ps, respectively [51]. The structural and thermodynamic properties of water inside the nanopores were then calculated from MD and NMPIMD simulations of 500 ps carried out in the NVT ensemble. The classical and quantum dynamical properties were obtained, respectively, from MD and CMD simulations of 100 ps carried out in the NVE ensemble.

In all cases, the equations of motion were propagated according to the velocity-Verlet algorithm with time steps $\Delta t = 0.2$ fs (NMPIMD), $\Delta t = 0.02$ fs (CMD) and $\Delta t = 0.5$ fs (MD) [51]. Massive Nosé–Hoover chains (NHCs) of four thermostats were employed in the NMPIMD and CMD simulations to ensure adequate canonical sampling [54]. In the CMD simulations, the centroid variables were propagated using the adiabatic separation scheme with an adiabaticity parameter $\gamma = 0.4$ [47], and NHCs of four thermostats were attached to each non-zero frequency normal mode. In all cases, the short-range interactions were truncated at an atom–atom distance of 12.0 Å, while the electrostatic interactions were treated using the Ewald sum [55].

## 3. Results and discussion

### *3.1 Structural properties*

As described in Ref. [37], MIL-53(Cr) undergoes two distinct transitions as a function of the number of water molecules adsorbed per unit cell. Figure 1 shows the variation in the unit cell volume obtained from classical NσT simulations carried out with the q-SPC/Fw model. The present results indicate that the nanopores remain open at $N_{H_2O} = 1$ and close at $N_{H_2O} = 2$. The material remains in the narrow pore configuration up to $N_{H_2O} \sim 5$ and slowly reopens between $N_{H_2O} = 6$ and $N_{H_2O} = 10$. A steep increase in the nanopore volume is then observed up to $N_{H_2O} = 14$ while the nanopore size of the empty framework is effectively recovered as $N_{H_2O} \rightarrow 20$. Figure 2 shows several snapshots extracted from the classical NσT simulations for different water loadings representing the instantaneous 3D distributions of the $H_2O$ molecules viewed along the framework nanochannels. For $N_{H_2O} = 1$, the present simulations indicate that the water molecules are preferentially arranged in four-membered cyclic

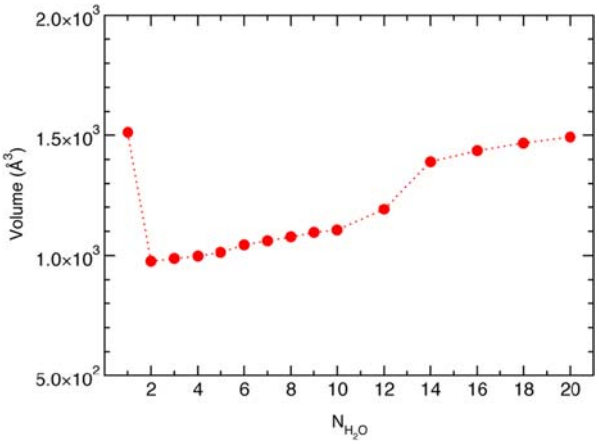


Figure 1. Variation in the MIL-53(Cr) unit cell volume as a function of the number of water molecules adsorbed, $N_{H_2O}$.

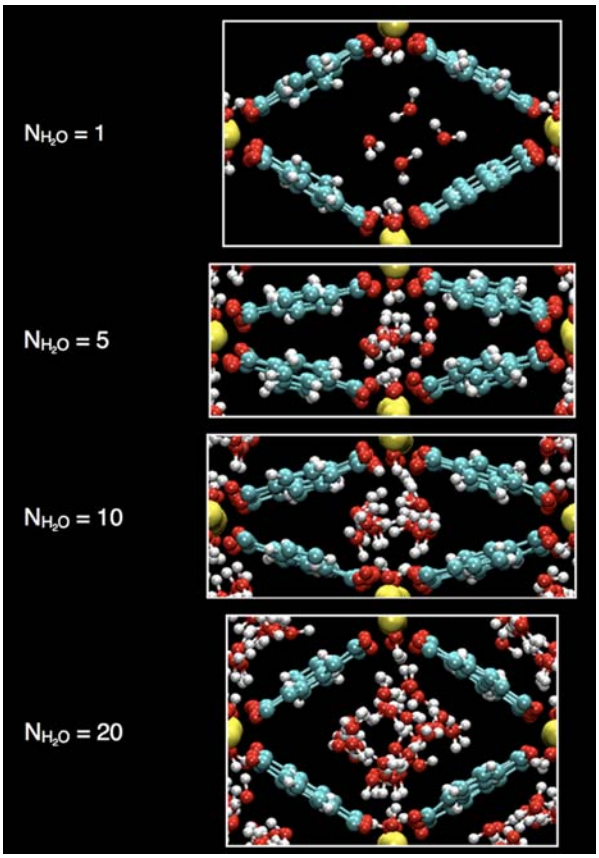


Figure 2. (Colour online) Three-dimensional snapshots extracted from the classical NσT simulations for different $N_{H_2O}$ values representing the instantaneous distributions of the water molecules viewed along the framework nanochannels.

clusters. However, since the water distribution in the nanopores at low loadings can be very inhomogeneous, other small clusters can also be formed depending on the actual number of molecules that are located within the same nanopore. When the MIL-53(Cr) structure closes into the narrow pore configuration (e.g. for $N_{H_2O} = 5$) the $H_2O$ molecules are preferentially aligned along the nanochannels effectively forming 1D hydrogen-bonded files where each water molecule accepts and donates one HB. Several water molecules located in favourable positions along the nanochannels also form a second HB with the oxygen atoms of the carboxylic groups of the framework. As $N_{H_2O}$ increases and, consequently, the nanopores open up, the structural arrangement of the $H_2O$ molecules becomes more disordered changing from approximately 1D files along the framework nanochannels to more spherical, 3D distributions within each nanopore. A similar spatial distribution of the water molecules, not shown, was also obtained from the corresponding NMPIMD simulations. Although the present results are in qualitative agreement with those reported in Ref. [37] from MD simulations with the TIP4P/2005 water model, some differences exist in the number of water molecules that are required for inducing the second structural transition that leads to the re-opening of the nanopores when $N_{H_2O} \geq 6$. This is likely due to the differences in the underlying water models as well as to the different initial distributions of the molecules used in the simulations. A detailed analysis of the effects of both water–water and water–framework interactions on the overall structural properties of MIL-53(Cr) will be reported in a forthcoming publication [56].

Direct insights into the impact of nuclear quantisation on the structural arrangements of water inside the nanopores of MIL-53(Cr) can be obtained from the analysis of the radial distribution functions (RDFs) describing the spatial correlations between the different atom pairs of the $H_2O$ molecules. In the present study, all RDFs are normalised to the total number of atomic species contained in the simulation box. Figure 3 shows the comparison between the classical and quantum oxygen–oxygen (O—O) RDFs calculated from MD and NMPIMD simulations, respectively, as a function of molecules adsorbed per unit cell. At low loadings, $N_{H_2O} \leq 3$, the two RDFs are essentially identical with the quantum

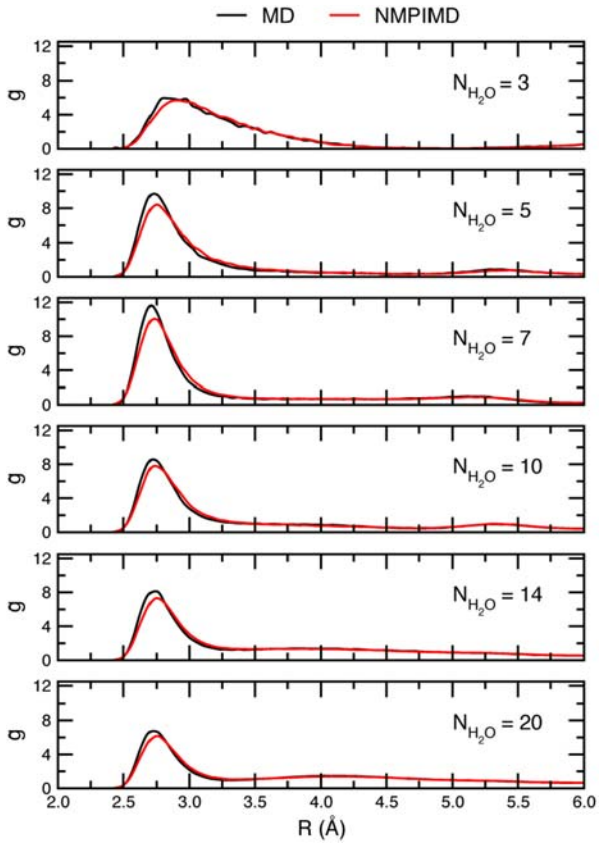


Figure 3. (Colour online) Comparison between the oxygen–oxygen RDFs obtained from MD (black) and NMPIMD (red) simulations for different water loadings, $N_{H_2O}$.

distribution being slightly shifted to larger distances by ~0.1 Å. This shift also persists at higher loadings and can be attributed to the effective larger volume occupied by the quantum $H_2O$ molecules due to the delocalisation arising from zero-point energy contributions. As $N_{H_2O}$ increases, the first peak located at ~2.7 Å, describing the correlation between the oxygen atoms of the molecules located within the first solvation shell, becomes more defined and a second peak starts building up as $N_{H_2O} \rightarrow 20$. At higher loadings, both O—O RDFs more closely resemble the corresponding distributions obtained for bulk water [53] with the establishment of a distinct second solvation shell at ~4.0 Å. For $N_{H_2O} > 3$ the first peak of the quantum O—O RDF is always broader and lower than the corresponding classical counterpart. This is a direct consequence of the atomic delocalisation resulting from the inclusion of nuclear quantisation, which effectively weakens the interaction between the water molecules as first described in Refs [57,58] (see Ref. [31] for a recent review).

Because of the light mass of the hydrogen atoms, the impact of nuclear quantum effects on the structural arrangement of the water molecules inside the MIL-53(Cr) nanopores becomes more visible when analysing the O—H and H—H RDFs shown in Figures 4 and 5, respectively. In both cases, appreciable differences exist in the shape of the first peak describing the spatial correlation between O and H atoms within the same $H_2O$ molecule. In both cases, the



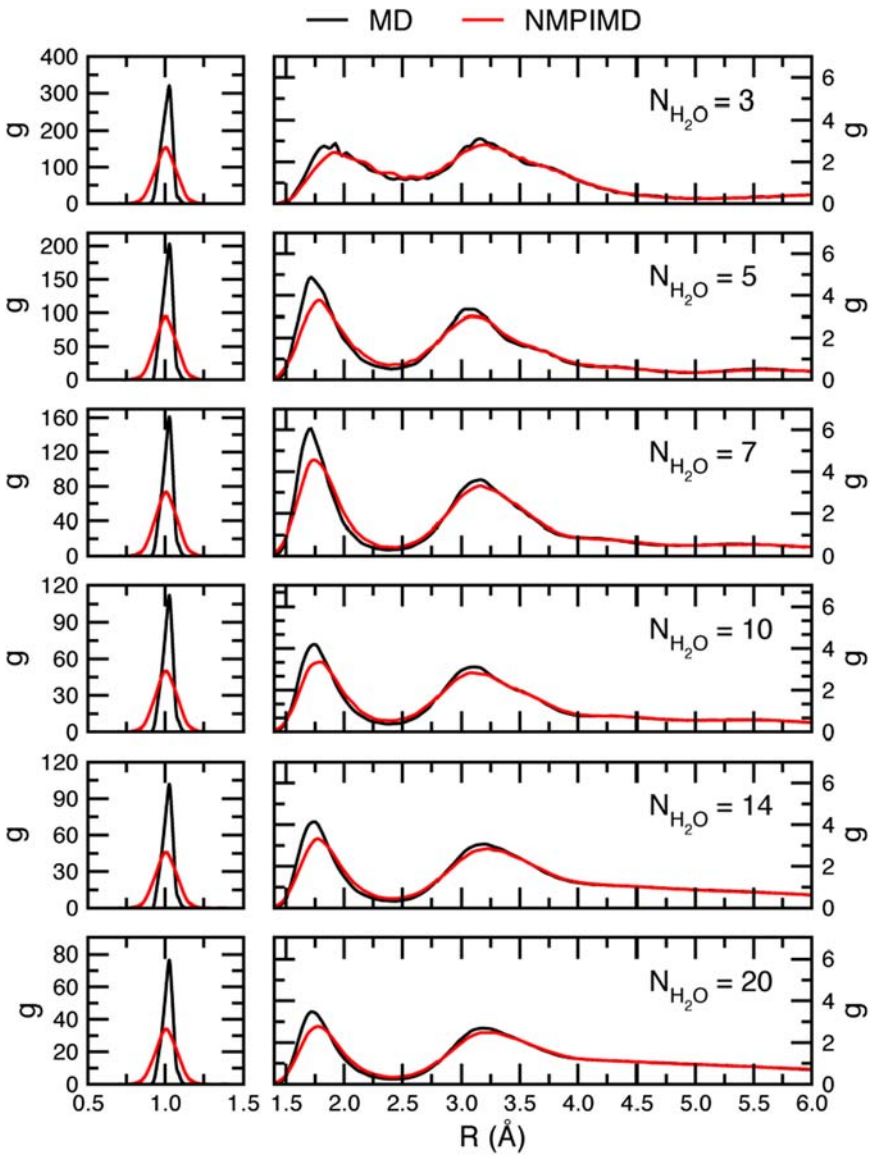


Figure 4. Comparison between the oxygen–hydrogen RDFs obtained from MD (black) and NMPIMD (red) simulations for different water loadings, $N_{H_2O}$.

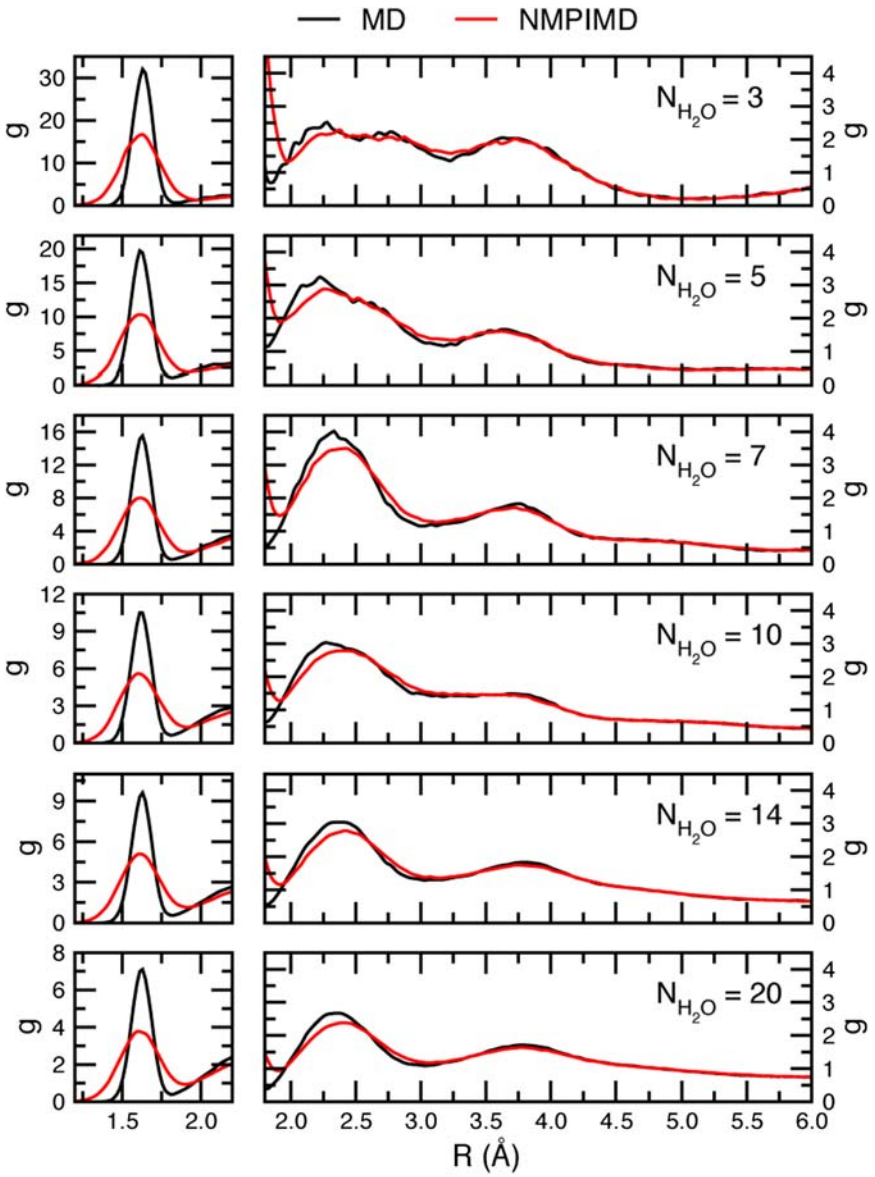


Figure 5. (Colour online) Comparison between the hydrogen–hydrogen RDFs obtained from MD (black) and NMPIMD (red) simulations for different water loadings, $N_{H_2O}$.

classical RDFs are significantly sharper due to the complete neglect of the zero-point energy. The differences between the classical and quantum results also persist at larger atomic separations. This is particularly evident in the O—H RDFs. Figure 4 shows that in the quantum distributions the second peak describing the spatial correlation between O and H atoms of different molecules that are partners in the same HB is always appreciably broader and shifted to larger distances. Small, but still noticeable, differences between the classical and quantum O—H RDFs are also found in the outer peak located at ~3.1 Å. This indicates that the impact of nuclear quantum effects on the structural arrangement of the $H_2O$ molecules extends beyond the first solvation shell. Overall, the RDFs calculated here for water adsorbed in MIL-53(Cr) are qualitatively similar to those obtained in Ref. [53] for bulk water, with the quantum distributions being always appreciably less structured than their classical counterparts.

In order to analyse the impact of nuclear quantisation on the dynamical properties of water confined in the MIL-53(Cr) nanopores, the classical and quantum self-diffusion coefficients were computed according to

$$D = \frac{1}{3}\int_0^\infty C_{vv}(t)\mathrm{d}t = \frac{1}{3}\int_0^\infty \langle v(t)v(0)\rangle \mathrm{d}t, \qquad (1)$$

where $C_{vv}(t)$ is the velocity autocorrelation function. While the classical $C_{vv}(t)$ can be calculated directly from MD simulations carried out in the NVE ensemble, the quantum counterpart was obtained from the corresponding Kubo transform derived from the CMD simulations [49,50]. A comparison between the classical and quantum diffusion coefficients as a function of $N_{H_2O}$ is reported in Table 1. Also listed there are the corresponding values obtained for bulk water [53]. For $N_{H_2O} = 1$, both the classical and quantum results indicate that the water diffusion is significantly faster than in the bulk. As discussed above, at this low loading, the MIL-53(Cr) nanopores remain open and the water molecules preferentially aggregate in small cyclic clusters. The fast water diffusion can thus be associated with the gas-like nature of these molecular complexes. For $2 \leq N_{H_2O} \leq 8$, MIL-53(Cr) closes into a narrow pore structure with the water molecules being arranged in 1D files along the nanochannels (Figure 1). This structural transition is accompanied by a drastic reduction in both classical and quantum diffusion coefficients. Interestingly, although the analysis of the RDFs suggests the presence of more loose HBs between the quantum $H_2O$ molecules, which generally implies a faster dynamics, the classical and quantum diffusion coefficients are essentially identical (within the statistical error). This behaviour is significantly different from that found in bulk water where the quantisation of the nuclear motion leads to an increase in water mobility by 40–50%. This difference can be attributed to the role played by the nanopores of MIL-53(Cr) that, at low water loading, create an extremely narrow confining environment. The latter effectively constrains the molecular motion and counteracts the effects associated with the nuclear quantisation, leading to an almost complete suppression of the water mobility.

Table 1. Diffusion coefficient calculated from MD and CMD simulations as a function of the number of water molecules adsorbed per unit cell.

| $N_{H_2O}$ | $D$ (Å$^2$ ps$^{-1}$) MD | $D$ (Å$^2$ ps$^{-1}$) CMD |
|---|---|---|
| 1 | 0.730 ± 0.01 | 0.810 ± 0.01 |
| 2 | 0.006 ± 0.01 | 0.002 ± 0.01 |
| 3 | 0.020 ± 0.01 | 0.030 ± 0.01 |
| 4 | 0.010 ± 0.01 | 0.030 ± 0.01 |
| 5 | 0.020 ± 0.01 | 0.040 ± 0.01 |
| 6 | 0.040 ± 0.01 | 0.040 ± 0.01 |
| 7 | 0.040 ± 0.01 | 0.060 ± 0.01 |
| 8 | 0.040 ± 0.01 | 0.040 ± 0.01 |
| 9 | 0.030 ± 0.01 | 0.030 ± 0.01 |
| 10 | 0.040 ± 0.01 | 0.040 ± 0.01 |
| 12 | 0.040 ± 0.01 | 0.060 ± 0.01 |
| 14 | 0.130 ± 0.01 | 0.160 ± 0.01 |
| 16 | 0.100 ± 0.01 | 0.160 ± 0.01 |
| 18 | 0.090 ± 0.01 | 0.100 ± 0.01 |
| 20 | 0.050 ± 0.01 | 0.060 ± 0.01 |
| Bulk | 0.170 ± 0.01 | 0.240 ± 0.01[a] |

[a] From Ref. [53].

Although the nanopores start opening at $N_{H_2O} = 6$ (Figures 1 and 2), the water diffusion coefficient remains extremely small up to $N_{H_2O} \sim 12$ when the unit cell volume of the empty framework is effectively recovered. For $12 \leq N_{H_2O} \leq 16$, the explicit account of nuclear quantisation results in a faster $H_2O$ diffusion, although D remains in all cases smaller than the corresponding bulk value. As the nanopores are filled up with water, the volume available to each molecule reduces, which is reflected in the reduction of the $H_2O$ mobility. As a consequence, D decreases for $N_{H_2O} > 16$ and the differences between the classical and quantum values become smaller.

Further insights into the impact of nuclear quantum effects on the properties of water adsorbed in the nanopores of MIL-53(Cr) are obtained from the analysis of the molecular rotational dynamics defined in terms of the orientational time autocorrelation function $C_2(t)$. Here, $C_2(t) = \langle P_2[\mathbf{e}(0)\cdot\mathbf{e}(t)]\rangle$ is the time autocorrelation function of the second-order Legendre polynomial $P_2[\mathbf{e}(0)\cdot\mathbf{e}(t)]$, where $\mathbf{e}(t)$ is a unit vector that lies along one of the two OH bonds of each $H_2O$ molecule. $C_2(t)$ is directly related to the anisotropy coefficient that can be measured in ultrafast vibrational pump-probe experiments [59,60]. A comparison between the classical and quantum $C_2(t)$ is shown in Figure 6 for different water loadings. Clearly, the rotational mobility of the water molecules is significantly affected by the shape of the nanopores. When MIL-53(Cr) is in the narrow pore configuration, the reorientation of the OH bonds is largely suppressed with $C_2(t)$ displaying, after an initial fast drop, an extremely slow decay. As $N_{H_2O}$ increases and the MIL-53(Cr) nanopores start opening, the rotational mobility of the $H_2O$ molecules also increases up to $N_{H_2O} = 16$ to decrease again as the nanopores are filled up with water. Interestingly, at low loadings (e.g. $N_{H_2O} = 3$), $C_2(t)$ displays multiple oscillations indicating that the water reorientation maintains some degree of coherence at relatively longer times (up to ~0.4 ps) than in bulk. This can be explained by considering that, since the dynamics in the narrow pores is effectively restricted in one dimension, the water molecules keep 'memory' of their past even after colliding with the other molecules and the framework. This implies that longer times than in the bulk phase are required before the orientational motion can become completely uncorrelated.

A more quantitative assessment of the impacts of nuclear quantisation on the water orientational dynamics can be derived from the analysis of the relaxation time, $\tau_2$, obtained from the exponential fit to the long time decay of $C_2(t)$. The comparison between the classical and quantum $\tau_2$ reported in Table 2 indicates that when the nanopores are closed the quantum reorientation of the OH bonds can become slower than its classical counterpart. This result is somewhat surprising since it is generally assumed that, by effectively weakening the molecular interactions, nuclear quantum effects lead to faster dynamics. However, as

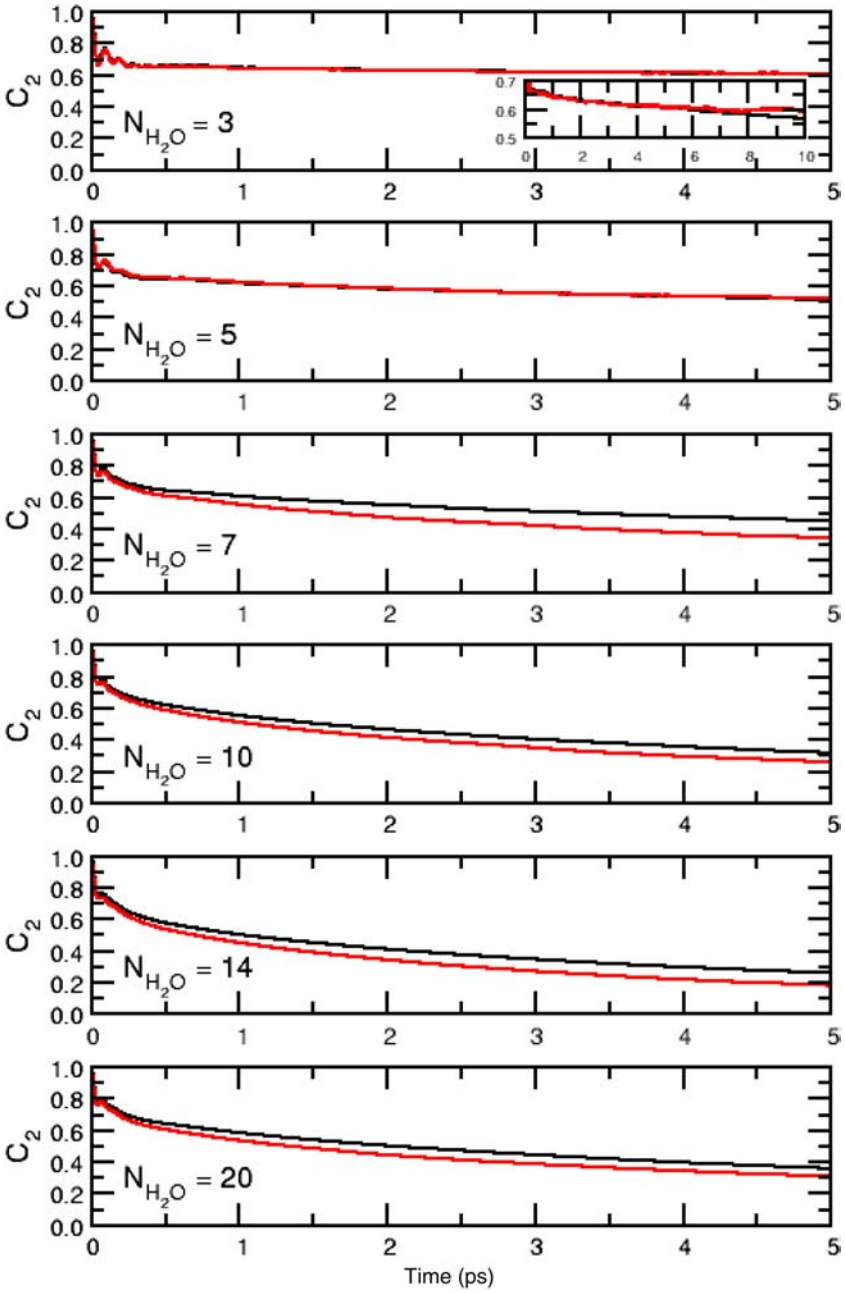


Figure 6. (Colour online) Comparison between the water orientational correlation functions obtained from MD (black) and CMD (red) simulations for different water loadings, $N_{H_2O}$.

mentioned above, the quantisation of the nuclear motion is accompanied by an effective increase in the molecular volume, which largely reduces the space available to the 'quantum' molecules in the nanopores especially when MIL-53(Cr) is in the narrow pore configuration. It is important to note that a more quantitative description of the water dynamics in the nanopores of MIL-53(Cr) would require more sophisticated models of the water–water and water–framework interactions as well as longer simulations. More specific studies along these lines will be reported in a forthcoming publication [56]. Nevertheless, the comparison between the ratio of $\tau_2$ calculated at the classical and quantum levels reported in the fourth column of Table 2 clearly indicates that, independently of the number of molecules adsorbed per unit cell, the confining environment created by the MIL-53(Cr) nanopores effectively counteracts the impact of nuclear quantisation on the water dynamics leading to a significant slowdown relative to bulk. In this context, it is interesting to note that quantum fluctuations have recently been shown to either promote or inhibit glass formation depending on the degree of 'quantumness' of the system [61].

Table 2. Relaxation time ($\tau_2$) associated with the decay of the orientational correlation function obtained from MD and CMD simulations as a function of the number of water molecules adsorbed per unit cell.

| $N_{H_2O}$ | $\tau_2$ (ps) MD | $\tau_2$ (ps) CMD | MD/CMD |
|---|---|---|---|
| 1 | 2.7 ± 0.1 | 2.9 ± 0.1 | 0.9 |
| 2 | 38.0 ± 0.1 | 41.5 ± 0.1 | 0.9 |
| 3 | 55.0 ± 0.1 | 61.8 ± 0.1 | 0.9 |
| 4 | 96.7 ± 0.1 | 161.8 ± 0.1 | 0.6 |
| 5 | 20.4 ± 0.1 | 20.4 ± 0.1 | 1.0 |
| 6 | 15.0 ± 0.1 | 12.3 ± 0.1 | 1.2 |
| 7 | 12.6 ± 0.1 | 7.8 ± 0.1 | 1.6 |
| 8 | 10.7 ± 0.1 | 8.9 ± 0.1 | 1.2 |
| 9 | 9.3 ± 0.1 | 7.2 ± 0.1 | 1.3 |
| 10 | 6.8 ± 0.1 | 5.5 ± 0.1 | 1.2 |
| 12 | 8.8 ± 0.1 | 6.3 ± 0.1 | 1.4 |
| 14 | 5.7 ± 0.1 | 4.2 ± 0.1 | 1.4 |
| 16 | 5.6 ± 0.1 | 4.2 ± 0.1 | 1.3 |
| 18 | 6.8 ± 0.1 | 5.2 ± 0.1 | 1.3 |
| 20 | 7.8 ± 0.1 | 6.8 ± 0.1 | 1.5 |
| Bulk | 3.3 ± 0.1 | 1.7 ± 0.1[a] | 1.9 |

Note: In the fourth column, the ratio between the classical and quantum results is also reported.[a] From Ref. [53].

The results reported in Table 2 also indicate that when the nanopores start opening and, consequently, more space becomes available, the explicit inclusion of nuclear quantum effects leads to a significantly faster orientational dynamics. As for the diffusion coefficient, a progressive slowdown of the water reorientation is then observed as the molecules fill up the nanopores. For both classical and quantum water $\tau_2$ is always smaller than the value obtained for bulk water. It is important to note that slightly different values were reported for classical water in Ref. [37]. These differences are likely due to the differences in the water models used in the simulations as well as to the different simulation procedures used in Ref. [37], where both $D$ and $\tau_2$ were obtained from NVT simulations.

## 4. Conclusions

The impact of nuclear quantum effects on the structural and dynamical properties of water adsorbed in the MIL-53(Cr) MOF was studied through classical and quantum MD simulations performed as a function of the water loading. The analysis of the spatial arrangement of the water molecules inside the nanopores shows that the explicit account of nuclear quantisation leads to less structured distributions indicating that the quantum molecules interact more weakly than their classical counterparts. Importantly, the RDFs calculated at the classical and quantum level for water in MIL-53(Cr) share many similarities with the corresponding functions obtained for bulk water, especially at higher loadings.

By contrast, large differences are found between the dynamical properties calculated at the classical and quantum levels. In particular, the present results indicate that, independently of the loading, the confining environment created by the nanopores of MIL-53(Cr) suppresses the mobility of the water molecules and largely reduces the impact of nuclear quantum effects. This is particularly evident in the orientational dynamics of the water molecules when MIL-53(Cr) is in the narrow pore configuration. In this case, the explicit quantisation of the nuclear motion leads to an extreme slowdown of the dynamics with the quantum molecules reorienting slower than their classical analogues. This is attributed to the larger volume occupied by the quantum $H_2O$ molecules, which is directly related to zero-point energy and atomic delocalisation. The increased molecular volume effectively reduces the free space available in the nanopores and, consequently, limits the water mobility.

Since the degree of delocalisation is inversely proportional to the temperature according to de Broglie's wavelength, it is expected that the slowdown of the dynamics of quantum water in the nanopores of MIL-53(Cr) will display a pronounced temperature dependence. In this regard, work is in progress in our group to determine the thermodynamic properties of water in MIL-53(Cr) as a function of both temperature and loading.

## Acknowledgements

This research was supported by start-up funds from the University of California at San Diego. We are grateful to the National Science Foundation for a generous allocation of computing time on Xsede resources as well as to the San Diego Supercomputer Center for a computing time allocation on the Triton Computing Cluster through the TAPP program.

## References

[1] O.M. Yaghi, M. O'Keeffe, N.W. Ockwig, H.K. Chae, M. Eddaoudi, and J. Kim, *Reticular synthesis and the design of new materials*, Nature 423 (2003), pp. 705–714.

[2] D.N. Dybtsev, H. Chun, and K. Kim, *Rigid and flexible: A highly porous metal-organic framework with unusual guest-dependent dynamic behavior*, Angew. Chem. Int. Ed. 43 (2004), pp. 5033–5036.

[3] C. Serre, F. Millange, C. Thouvenot, M. Nogues, G. Marsolier, D. Louer, and G. Ferey, *Very large breathing effect in the first nanoporous chromium(III)-based solids: MIL-53 or Cr-III(OH)({O$_2$C-C$_6$H$_4$-CO$_2$}({HO$_2$C-C$_6$H$_4$-CO$_2$H}(x)·H$_2$Oy*, J. Am. Chem. Soc. 124 (2002), pp. 13519–13526.

[4] T. Loiseau, C. Serre, C. Huguenard, G. Fink, F. Taulelle, M. Henry, T. Bataille, and G. Ferey, *A rationale for the large breathing of the porous aluminum terephthalate (MIL-53) upon hydration*, Chem. Eur. J. 10 (2004), pp. 1373–1382.

[5] N.A. Ramsahye, G. Maurin, S. Bourrelly, P.L. Llewellyn, T. Loiseau, C. Serre, and G. Ferey, *On the breathing effect of a metal-organic framework upon $CO_2$ adsorption: Monte Carlo compared to microcalorimetry experiments*, Chem. Commun. (2007), pp. 3261–3263.

[6] P. Horcajada, C. Serre, G. Maurin, N.A. Ramsahye, F. Balas, M. Vallet-Regi, M. Sebban, F. Taulelle, and G. Ferey, *Flexible porous metal-organic frameworks for a controlled drug delivery*, J. Am. Chem. Soc. 130 (2008), pp. 6774–6780.

[7] P.L. Llewellyn, G. Maurin, T. Devic, S. Loera-Serna, N. Rosenbach, C. Serre, S. Bourrelly, P. Horcajada, Y. Filinchuk, and G. Ferey, *Prediction of the conditions for breathing of metal organic framework materials using a combination of X-ray powder diffraction, microcalorimetry, and molecular simulation*, J. Am. Chem. Soc. 130 (2008), pp. 12808–12814.

[8] S. Shimomura, S. Horike, R. Matsuda, and S. Kitagawa, *Guest-specific function of a flexible undulating channel in a 7,7,8,8-tetracyano-p-quinodimethane dimer-based porous coordination polymer*, J. Am. Chem. Soc. 129 (2007), pp. 10990–10991.

[9] S. Shimomura, R. Matsuda, and S. Kitagawa, *Flexibility of porous coordination polymers strongly linked to selective sorption mechanism*, Chem. Mater. 22 (2010), pp. 4129–4131.

[10] S. Shimomura, M. Higuchi, R. Matsuda, K. Yoneda, Y. Hijikata, Y. Kubota, Y. Mita, J. Kim, M. Takata, and S. Kitagawa, *Selective sorption of oxygen and nitric oxide by an electron-donating flexible porous coordination polymer*, Nat. Chem. 2 (2010), pp. 633–637.

[11] S. Horike, S. Shimomura, and S. Kitagawa, *Soft porous crystals*, Nat. Chem. 1 (2009), pp. 695–704.

[12] Z.Q. Wang and S.M. Cohen, *Modulating metal-organic frameworks to breathe: A postsynthetic covalent modification approach*, J. Am. Chem. Soc. 131 (2009), pp. 16675–16677.

[13] T. Devic, P. Horcajada, C. Serre, F. Salles, G. Maurin, B. Moulin, D. Heurtaux, G. Clet, A. Vimont, J.M. Greneche, B. Le Ouay, F. Moreau, E. Magnier, Y. Filinchuk, J. Marrot, J.C. Lavalley, M. Daturi, and G. Ferey, *Functionalization in flexible porous solids: Effects on the pore opening and the host-guest interactions*, J. Am. Chem. Soc. 132 (2010), pp. 1127–1136.

[14] G. Ferey, *Hybrid porous solids: Past, present, future, Chem*, Soc. Rev. 37 (2008), pp. 191–214.

[15] J.R. Long and O.M. Yaghi, *The pervasive chemistry of metal-organic frameworks*, Chem. Soc. Rev. 38 (2009), pp. 1213–1214.

[16] G. Ferey, C. Serre, T. Devic, G. Maurin, H. Jobic, P.L. Llewellyn, G. De Weireld, A. Vimont, M. Daturi, and J.S. Chang, *Why hybrid porous solids capture greenhouse gases?* Chem. Soc. Rev. 40 (2011), pp. 550–562.

[17] J.A. Greathouse and M.D. Allendorf, *The interaction of water with MOF-5 simulated by molecular dynamics*, J. Am. Chem. Soc. 128 (2006), pp. 10678–10679.

[18] K.S. Park, Z. Ni, A.P. Cote, J.Y. Choi, R.D. Huang, F.J. Uribe-Romo, H.K. Chae, M. O'Keeffe, and O.M. Yaghi, *Exceptional chemical and thermal stability of zeolitic imidazolate frameworks*, Proc. Natl. Acad. Sci. USA 103 (2006), pp. 10186–10191.

[19] A. Demessence, D.M. D'Alessandro, M.L. Foo, and J.R. Long, *Strong $CO_2$ binding in a water-stable, triazolate-bridged metal-organic framework functionalized with ethylenediamine*, J. Am. Chem. Soc. 131 (2009), pp. 8784–8786.

[20] Y. Li and R.T. Yang, *Gas adsorption and storage in metal-organic framework MOF-177*, Langmuir 23 (2007), pp. 12937–12944.

[21] A. Kondo, T. Daimaru, H. Noguchi, T. Ohba, K. Kaneko, and H. Kanob, *Adsorption of water on three-dimensional pillared-layer metal organic frameworks*, J. Colloid Interface Sci. 314 (2007), pp. 422–426.

[22] P. Kusgens, M. Rose, I. Senkovska, H. Frode, A. Henschel, S. Siegle, and S. Kaskel, *Characterization of metal-organic frameworks by water adsorption*, Microporous Mesoporous Mater. 120 (2009), pp. 325–330.

[23] J.J. Low, A.I. Benin, P. Jakubczak, J.F. Abrahamian, S.A. Faheem, and R.R. Willis, *Virtual high throughput screening confirmed experimentally: Porous coordination polymer hydration*, J. Am. Chem. Soc. 131 (2009), pp. 15834–15842.

[24] S.S. Han, S.H. Choi, and A.C. van Duin, *Molecular dynamics simulations of stability of metal-organic frameworks against $H_2O$ using the ReaxFF reactive force field*, Chem. Commun. (Camb.) 46 (2010), pp. 5713–5715.

[25] Z.X. Chen, S.C. Xiang, D.Y. Zhao, and B.L. Chen, *Reversible two-dimensional-three dimensional framework transformation within a prototype metal-organic framework*, Cryst. Growth Des. 9 (2009), pp. 5293–5296.

[26] A.R. Millward and O.M. Yaghi, *Metal-organic frameworks with exceptionally high capacity for storage of carbon dioxide at room temperature*, J. Am. Chem. Soc. 127 (2005), pp. 17998–17999.

[27] A.O. Yazaydin, A.I. Benin, S.A. Faheem, P. Jakubczak, J.J. Low, R.R. Willis, and R.Q. Snurr, *Enhanced $CO_2$ adsorption in metal-organic frameworks via occupation of open-metal sites by coordinated water molecules*, Chem. Mater. 21 (2009), pp. 1425–1430.

[28] M.A. Ricci, F. Bruni, P. Gallo, M. Rovere, and A.K. Soper, *Water in confined geometries: Experiments and simulations*, J. Phys. Condens. Matter 12 (2000), pp. A345–A350.

[29] J.C. Rasaiah, S. Garde, and G. Hummer, *Water in nonpolar confinement: From nanotubes to proteins and beyond*, Annu. Rev. Phys. Chem. 59 (2008), pp. 713–740.

[30] H.K. Christenson, *Confinement effects on freezing and melting*, J. Phys. Condens. Matter 13 (2001), pp. R95–R133.

[31] F. Paesani and G.A. Voth, *The properties of water: Insights from quantum simulations*, J. Phys. Chem. B 113 (2009), pp. 5702–5719.

[32] L. Hernández de la Peña and P.G. Kusalik, *Temperature dependence of quantum effects in liquid water*, J. Am. Chem. Soc. 127 (2005), pp. 5246–5251.

[33] F. Millange, C. Serre, and G. Ferey, *Synthesis, structure determination and properties of MIL-53as and MIL-53ht: The first Cr-III hybrid inorganic-organic microporous solids: Cr-III(OH)·{$O_2$C-$C_6H_4$-$CO_2$}·{$HO_2$C-$C_6H_4$-$CO_2$H}$_x$*, Chem. Commun. (2002), pp. 822–823.

[34] S. Bourrelly, P.L. Llewellyn, C. Serre, F. Millange, T. Loiseau, and G. Ferey, *Different adsorption behaviors of methane and carbon dioxide in the isotypic nanoporous metal terephthalates MIL-53 and MIL-47*, J. Am. Chem. Soc. 127 (2005), pp. 13519–13521.

[35] D.S. Coombes, F. Cora, C. Mellot-Draznieks, and R.G. Bell, *Sorption-induced breathing in the flexible metal organic framework CrMIL-53: Force-field simulations and electronic structure analysis*, J. Chem. Phys. C 113 (2008), pp. 544–552.

[36] F. Salles, A. Ghoufi, G. Maurin, R.G. Bell, C. Mellot-Draznieks, and G. Ferey, *Molecular dynamics simulations of breathing MOFs: Structural transformations of MIL-53(Cr) upon thermal activation and $CO_2$ adsorption*, Angew. Chem. Int. Ed. 47 (2008), pp. 8487–8491.

[37] F. Salles, S. Bourrelly, H. Jobic, T. Devic, V. Guillerm, P. Llewellyn, C. Serre, G. Ferey, and G. Maurin, *Molecular insight into the adsorption and diffusion of water in the versatile hydrophilic/hydrophobic flexible MIL-53(Cr) MOF*, J. Phys. Chem. C 115 (2011), pp. 10764–10776.

[38] F. Salles, H. Jobic, A. Ghoufi, P.L. Llewellyn, C. Serre, S. Bourrelly, G. Ferey, and G. Maurin, *Transport diffusivity of $CO_2$ in the highly flexible metal-organic framework MIL-53(Cr)*, Angew. Chem. Int. Ed. 48 (2009), pp. 8335–8339.

[39] L. Hamon, H. Leclerc, A. Ghoufi, L. Oliviero, A. Travert, J.C. Lavalley, T. Devic, C. Serre, G. Ferey, G. De Weireld, A. Vimont, and G. Maurin, *Molecular insight into the adsorption of $H_2S$ in the flexible MIL-53(Cr) and rigid MIL-47(V) MOFs: Infrared spectroscopy combined to molecular simulations*, J. Phys. Chem. C 115 (2011), pp. 2047–2056.

[40] M. Parrinello and A. Rahman, *study of An F-Center in molten KCl*, J. Chem. Phys. 80 (1984), pp. 860–867.

[41] G.A. Voth, *Path integral centroid methods in quantum statistical mechanics and dynamics*, Adv. Chem. Phys. 93 (1996), pp. 135–218.

[42] R.P. Feynman and A.R. Hibbs, *Quantum Mechanics and Path Integrals*, McGraw-Hill, New York, 1965.

[43] R.P. Feynman, *Statistical Mechanics*, Benjamin, New York, 1972.

[44] J. Cao and G.A. Voth, *The formulation of quantum-statistical mechanics based on the Feynman path centroid density. 1. Equilibrium properties*, J. Chem. Phys. 100 (1994), pp. 5093–5105.

[45] J. Cao and G.A. Voth, *The formulation of quantum-statistical mechanics based on the Feynman path centroid density. 2. Dynamical properties*, J. Chem. Phys. 100 (1994), pp. 5106–5117.

[46] J. Cao and G.A. Voth, *The formulation of quantum-statistical mechanics based on the Feynman path centroid density. 3. Phase-space formalism and analysis of centroid molecular-dynamics*, J. Chem. Phys. 101 (1994), pp. 6157–6167.

[47] J. Cao and G.A. Voth, *The formulation of quantum-statistical mechanics based on the Feynman path centroid density. 4. Algorithms for centroid molecular-dynamics*, J. Chem. Phys. 101 (1994), pp. 6168–6183.

[48] J. Cao and G.A. Voth, *The formulation of quantum-statistical mechanics based on the Feynman path centroid density. 5. Quantum instantaneous normal-mode theory of liquids*, J. Chem. Phys. 101 (1994), pp. 6184–6192.
[49] S. Jang and G.A. Voth, *Path integral centroid variables and the formulation of their exact real time dynamics*, J. Chem. Phys. 111 (1999), pp. 2357–2370.
[50] S. Jang and G.A. Voth, *A derivation of centroid molecular dynamics and other approximate time evolution methods for path integral centroid variables*, J. Chem. Phys. 111 (1999), pp. 2371–2370.
[51] D. Frenkel and B. Smit, *Understanding Molecular Simulation: From Algorithms to Applications*, Academic Press, San Diego, 2001.
[52] M.E. Tuckerman, *Statistical Mechanics: Theory and Molecular Simulation*, Oxford University Press, Oxford, 2010.
[53] F. Paesani, W. Zhang, D.A. Case, T.E. Cheatham, III, and G.A. Voth, *An accurate and simple quantum model for liquid water*, J. Chem. Phys. 125 (2006), 184507.
[54] G.J. Martyna, M.L. Klein, and M. Tuckerman, *Nosé-Hoover chains – The canonical ensemble via continuous dynamics*, J. Chem. Phys. 97 (1992), pp. 2635–2643.
[55] M.P. Allen and D.J. Tildesley, *Computer Simulations of Liquids*, Clarendon, Oxford, 1987.
[56] P. Howland, J.C. Sung, and F. Paesani, *Polarization effects in the adsorption of water in MIL-53(Cr)*, submitted (2012)
[57] R.A. Kuharski and P.J. Rossky, *A quantum-mechanical study of structure in liquid $H_2O$ and $D_2O$*, J. Chem. Phys. 82 (1985), p. 5164.
[58] A. Wallqvist and B.J. Berne, *Path-integral simulation of pure water*, Chem. Phys. Lett. 117 (1985), pp. 214–219.
[59] H.J. Bakker and J.L. Skinner, *Vibrational spectroscopy as a probe of structure and dynamics in liquid water*, Chem. Rev. 110 (2010), pp. 1498–1517.
[60] F. Paesani S. Yoo, H.J. Bakker, and S.S. Xantheas, *Nuclear quantum effects in the reorientation of water*, J. Phys. Chem. Lett. 1 (2010), pp. 2316–2321.
[61] T.E. Markland, J.A. Morrone, B.J. Berne, K. Miyazaki, E. Rabani, and D.R. Reichman, *Quantum fluctuations can promote or inhibit glass formation*, Nat. Phys. 7 (2011), pp. 134–137\.